Heterolytic splitting of H–X bonds at a cationic (PNP)Pd center†

Lauren C. Gregor,[a] Chung-Hsing Chen,[a] Claudia M. Fafard,[a] Lei Fan,[a] Chengyun Guo,[a] Bruce M. Foxman,[a] Dmitry G. Gusev[b] and Oleg V. Ozerov*[a,c]

Received 2nd December 2009, Accepted 2nd February 2010
First published as an Advance Article on the web 3rd March 2010
DOI: 10.1039/b925265g

The (PNP)PdOTf complex is a suitable synthetic equivalent of the $[(PNP)Pd]^+$ fragment in reactions with various HX substrates. The $[(PNP)Pd]^+$ fragment either simply binds HX molecules as L-type ligands (X = NH_2, PCy_2, imidazolyl) or heterolytically splits the H–X bond to produce $[(PN(H)P)Pd–X]^+$ (X = H, CCR, SR). DFT calculations analyze the relative energetics of the two outcomes and agree with the experimental data. Calculations also allow to assess the unobserved Pd(IV) isomer $[(PNP)Pd(H)_2]^+$ and validate its unfavourability with respect to the Pd(II) isomer $[(PN(H)P)PdH]^+$.

Introduction

Addition of hydrogen-element (H–X) bonds to transition metal complexes is of central importance in organometallic chemistry. Addition of H–X to a metal center with formation of new M–H and M–X bonds is a classical oxidative addition reaction (Scheme 1).[1] 1,2-addition across a metal–ligand bond (M–Y) is also possible and is typically accomplished at the expense of a metal ligand π-bond. Classical oxidative addition requires both a filled and an empty orbital at the same transition metal center (or a main group element; *e.g.*, in a carbene)[2] and proceeds with a change of oxidation state of the metal center. A 1,2-addition utilizes a ligand-based pair of electrons and an empty orbital at the metal and proceeds without a change in oxidation state. Addition of H–H across a $Ru–N_{amido}$ bond is a key mechanistic step in the Noyori-type hydrogenation.[3,4] Examples of multiple metal ligand bonds that perform addition of even unreactive C–H bonds in alkanes are known and include group 6 metal alkylidenes,[5] group 4 metal imido complexes,[6] and Ti alkylidynes.[7]

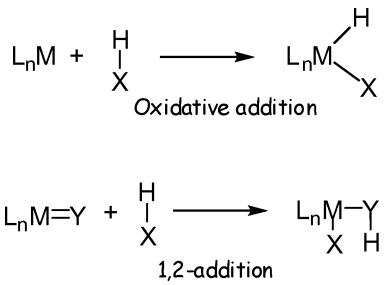

Scheme 1 Oxidative addition to a metal center and the non-oxidative 1,2-addition.

In the present work, we report our investigations of addition of various H–X substrates across a Pd–N moiety in a cationic, three-coordinate $[(PNP)Pd]^+$ fragment where PNP is a diarylamido/bis(phosphine) pincer ligand (Scheme 2).[8] In contrast to Ru amides in the Noyori cycle,[3,4] Legzdins metal alkylidenes,[5] Wolczanski's metal imides,[6] and Mindiola's Ti alkylidyne,[7] the $[(PNP)Pd]^+$ fragment should not contain a Pd–N π-bond because all orbitals of d_π-symmetry at Pd are filled. Instead, it contains a nitrogen-based lone pair (albeit delocalized over the diarylamide π-system) and a σ-symmetry empty orbital at Pd

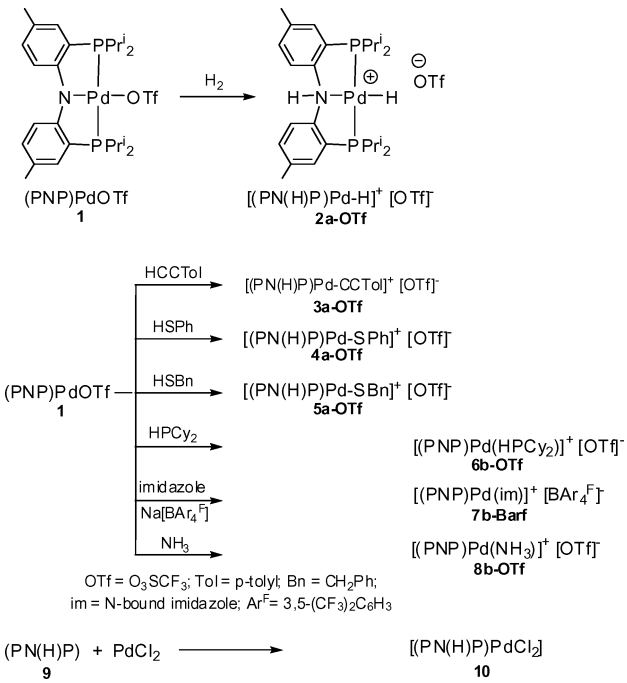

Scheme 2 Reactions of various H–X substrates with (PNP)PdOTf (**1**) in benzene or toluene.

[a]*Department of Chemistry, Brandeis University, 415 South Street, Waltham, MA 02454, USA*
[b]*Department of Chemistry, Wilfrid Laurier University, Waterloo, Ontario N2L 3C5, Canada*
[c]*Department of Chemistry, Texas A&M University, College Station, TX 77842, USA. E-mail: ozerov@mail.chem.tamu.edu*

† Electronic supplementary information (ESI) available: Coordinate tables for the calculated structures, selected pictorial NMR spectra and representations of calculated molecular orbitals. CCDC reference numbers 756641–756644. For ESI and crystallographic data in CIF or other electronic format see DOI: 10.1039/b925265g

(corresponding to the site of the "missing" fourth ligand of a square planar complex). The formation of a π-bond is precluded by the orthogonality of the lone pair and the empty orbital that is enforced by the pincer ligand, while intermolecular σ-bond formation (*i.e.*, di- or oligomerization) is presumably unfavourable for steric reasons. From this perspective, the $[(PNP)Pd]^+$ fragment is related to the so-called frustrated Lewis acid–base pairs that has been recently reinvigorated by Stephan *et al.*[9] Addition of H_2 to complexes of a PNP* ligand derived from deprotonated bis(phosphinomethyl)pyridine described by Milstein *et al.* is also conceptually similar.[10] In the present work, we describe a series of experiments with various H–X substrates and analyze the heterolytic H-X splitting as well as other possible reaction outcomes.

Results and discussion

Synthesis of cationic H–X adducts

We chose (PNP)PdOTf (**1**) as a synthon for $[(PNP)Pd]^+$. The synthesis of **1** was previously reported.[11] Compound **1** itself is a molecular compound in non-polar solvents, but triflate is a weakly enough coordinated ligand that it can be displaced by some neutral ligands. We previously showed that the 3d metal analog, (PNP)NiOTf, reacts with acetonitrile to form a cationic acetonitrile complex and is an active catalyst for nitrile/aldehyde coupling.[12]

Several H–X substrates (Scheme 2) were selected for the study. Reactions were performed by adding 1.0–1.2 equiv. of a substrate to **1** in an aromatic solvent, with the exception of H_2 and NH_3 which were added in excess (1 atm). In cases where displacement of triflate did take place, the new ionic products were easily isolated in analytical purity and good yields even on an NMR tube scale. No change was observed by *in situ* NMR analysis in reactions with pyrrole, acetylacetone, acetic acid, and ethanol, even after the solutions were subjected to thermolysis at 100 °C overnight.

The reactions with H_2, HCCTol, HSPh, and $HSCH_2Ph$ led to the transformation of the dark-blue colour of **1** to colourless (**2a-OTf**), yellow (**3a-OTf**), or red (**4a-OTf**, **5a-OTf**). With H_2 the colour change took place over 10 min; for the other three substrates, it was complete within the time of mixing. The products **2/3/4/5a-OTf** show spectroscopic characteristics consistent with the addition of the H–X bond across the N–Pd bond. Each displayed an N–H resonance in the δ 10.5–11.5 ppm region of the ^{1}H NMR spectra and a signal at around −80.5 ppm in the ^{19}F NMR spectra attributed to free triflate. The NMR spectra also contained appropriate resonances arising from the X group bound to Pd. Most tellingly, **2a-OTf** displayed a Pd–H resonance at δ −12.05 ppm.

The (PNP)Pd fragment of **1** possesses C_2 symmetry but appears C_{2v} symmetrical on the NMR timescale due to a combination of torsional and rotational motions involving the ligand backbone and the ^{i}Pr groups. Addition of a proton to the N of PNP destroys the rotational symmetry and makes the $[(PN(H)P)PdX]^+$ complexes appear C_s symmetrical in solution. All compounds **2/3/4/5a-OTf** possess effective C_s symmetry as observed in the ^{1}H and ^{13}C NMR spectra at ambient temperature.

While we have not performed a reaction of HCl with **1** here, several years ago we reported on the reaction of (PN(H)P) (**9**) with $PdCl_2$, which produced $(PN(H)P)PdCl_2$ **10** (Scheme 2).[13] The exact structure of **10** was not determined, but the presence of NH could be inferred from the downfield resonance in the ^{1}H NMR spectrum. Thus we can tentatively view **10** as an adduct of HCl across the N–Pd bond in $[(PNP)Pd]^+$ (if only one chloride in **10** is coordinated to Pd) or in (PNP)PdCl (if both chlorides in **10** are Pd-bound).

Reactions with $HPCy_2$ and imidazole led to rapid color change from the dark blue of **1** to different shades of purple. The solubility of the product of the reaction of imidazole with **1** (**7b-OTf**) was poor and we chose to isolate the more soluble $BAr^F{}_4$ salt (**7b-Barf**) *via* simple salt metathesis. The products of these reactions did not show any ^{1}H NMR resonances in the 10-11 ppm range, indicating the absence of H on the N of PNP. On the contrary, the ^{1}H NMR spectrum of **6b-OTf** contained a diagnostic doublet at δ 4.78 ppm with $^1J_{HP} = 352$ Hz, indicating the preservation of the P–H bond. A phosphorus-phosphorus coupling constant of 34 Hz was evident in the AX_2 system in the $^{31}P\{^1H\}$ spectrum of **6b-OTf**. The NMR spectra of **7b-Barf** and the other features of the spectra of **6b-OTf** were also consistent with a simple adduct formation; for example, C_{2v} symmetry was maintained. The reaction with NH_3 was reported previously and gave a similar product (**8b-OTf**).[14]

Deprotonation of the cationic H–X adducts

Deprotonation of complexes **2a/3a/4a/5a/6b/8b-OTf** was carried out in a straightforward fashion (Scheme 3). Addition of a Brønsted base to a solution of the cationic complex resulted in the formation of the corresponding (PNP)PdX complexes (**2x-6x** and **8x**). We did not attempt to optimize the strength of the base required to deprotonate different compounds, however, it is worth noting that the complexes containing a protonated PNP ligand were deprotonated by rather weak bases.

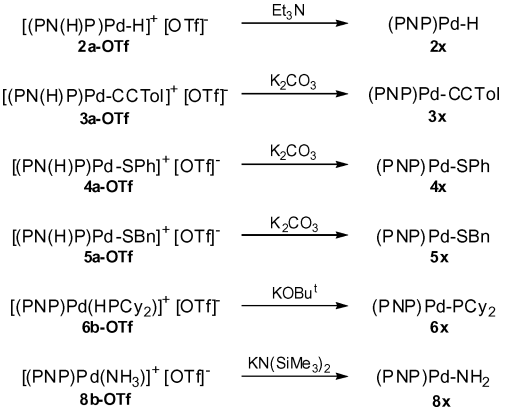

Scheme 3 Deprotonation of cationic HX adducts.

Complexes **2x-6x** and **8x** give rise to C_{2v}-symmetric NMR spectra that are typical for (PNP)PdX complexes. Complex **6x** displays an AX_2 system ($J_{PP} = 21$ Hz) in its $^{31}P\{^1H\}$ spectrum, consistent with a disposition of the dialkylphosphide ligand *cis*- to the phosphines of PNP.

Solid state structures determined by X-ray diffraction

We were able to obtain quality single crystals for compounds **2a-OTf**, **3x**, **6x**, and **7b-Barf** that were suitable for X-ray diffraction

studies. The ORTEP representations of the molecular structures in the solid state are given in Fig. 1–4. Compound **2a-OTf** represents the first structure of a PN(H)P ligand with any metal. The triflate anion in **2a-OTf** is not coordinated to Pd, but is involved in a hydrogen bond with the NH proton. The other three structures contain a PNP ligand with a central amido, sp^2-hybridized nitrogen donor. The bond distances and angles associated with the (PNP)Pd system in **3x**, **6x**, and **7b-Barf** are unremarkable and are within the range of values reported for other PNP complexes of Pd. In fact, the metrics associated with the phosphines of PNP are similar across all four compounds: the P–Pd–P angle varies within the *ca.* 160–169° range while the average Pd–P distances range from *ca.* 2.27 Å to *ca.* 2.32 Å. The differences are slight and likely caused primarily by the magnitude of steric repulsion with the fourth ligand in the coordination plane of Pd.

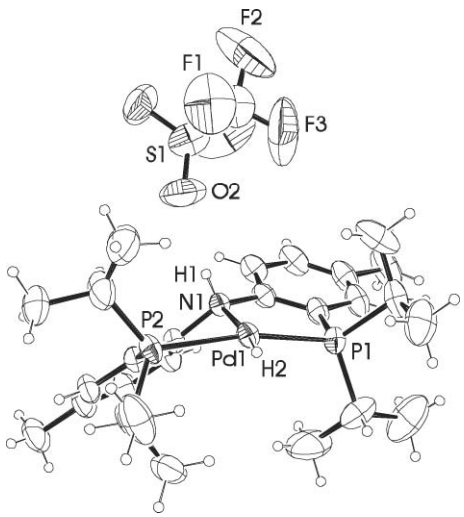

Fig. 1 ORTEP drawing (30% probability ellipsoids) of **2a-OTf** showing selected atom labelling. Selected interatomic distances (Å) and angles (°) follow: Pd1–P1, 2.2465(9); Pd1–P2, 2.2854(9); Pd1–N1, 2.164(3); Pd1–H2, 1.543; N1–H1, 0.86(5); O2···N1, 2.833(6); P1–Pd1–P2, 162.05(4); N1–Pd1–H2, 176.6; N1–H1···O2, 172(4).

The geometry about the P3 phosphorus atom of the PCy_2 unit in **6x** is distinctly pyramidal, indicative of sp^3-hybridization at this P atom. The Pd1–P3 distance of 2.3493(5) Å is comparable to the Pd–P_{PNP} bond lengths. These facts are consistent with a purely single bond character for the Pd–PCy_2 bond. A square planar Pd(II) center lacks empty d-orbitals of appropriate symmetry to support a π-bond with the phosphide. Other examples of structurally characterized square planar Pd(II) phosphido complexes also display a pyramidalized phosphide phosphorus atom and relatively long Pd–P bond distances.[15,16]

The trend in Pd–N_{PNP} distances can be rationalized by invoking *trans*-influence arguments. The shortest Pd–N_{PNP} distance of 2.008(4) Å was observed in **7b-Barf**, followed by 2.062(3) Å in **3x** (CCAr) and 2.1186(15) in **6x** (PCy_2). That the order of apparent *trans*-influence is imidazole < $^-$CCR < $^-PCy_2$ is quite reasonable; this is also the order of increasing Brønsted basicity. Interestingly, the Pd–N_{PNP} bond length in **7b-Barf** is the shortest we have recorded so far with this type of the PNP ligand, while that in **6x** is the longest. For comparison, the Pd–N_{PNP} distance

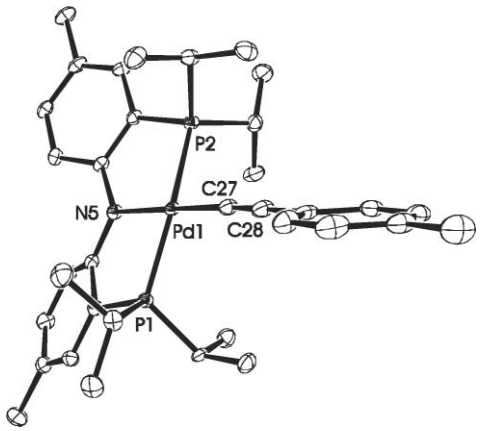

Fig. 2 ORTEP drawing (50% probability ellipsoids) of **3x** showing selected atom labelling. Hydrogen atoms are omitted for clarity. Selected bond distances (Å) and angles (°) follow: Pd1–P1, 2.2574(8); Pd1–P2, 2.2746(8); Pd1–N5, 2.062(3); Pd1–C27, 1.984(3); C27–C28, 1.191(5); P1–Pd1–P2, 168.39(3); N5–Pd1–C27, 176.79(12).

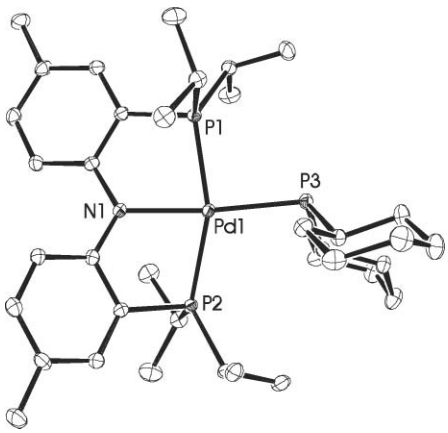

Fig. 3 ORTEP drawing (50% probability ellipsoids) of **6x** showing selected atom labelling. Hydrogen atoms are omitted for clarity. Selected bond distances (Å) and angles (°) follow: Pd1–P1, 2.2964(5); Pd1–P2, 2.3410(5); Pd1–P3, 2.3494(5); Pd1–N1, 2.1186(15); P1–Pd1–P2, 160.661(17); N1–Pd1–P3, 174.34(4).

in (^{F}PNP)PdMe[17] is 2.0938(15) Å and that in (PNP)PdCl is 2.0258(19) Å.[13] The Pd–N_{PNP} distance in **2a-OTf** is notably longer at 2.160(4) Å because the nitrogen donor in it is an amine and also because it is *trans* to the strongly *trans* influencing hydride.

Computational studies and analysis

In order to assist our understanding of the reactivity preferences of the H–X molecules under study, we carried out a computational study of a series of relevant substrates. DFT methods were used to optimize the geometries and obtain gas-phase energies of either the conventional H–X adducts of $[(PNP)Pd]^+$ or the products of H–X addition across the N–Pd bond in $[(PNP)Pd]^+$. Properties computed in the gas phase for ionic species may deviate significantly from the solution properties. However, here we undertake a comparison between two isomeric cations where much of the solution *vs.* gas phase discrepancy can be expected to cancel out.

Table 1 DFT calculated enthalpies[a] of the isomerization reaction $[(PNP)Pd(XH)]^+ \rightarrow [(PN(H)P)PdX]^+$

#	XH	ΔH / kcal mol^{-1}
1	H_2	−16.8
2	CH_4	−7.5
3	HC≡CH	−5.6
4	HC≡CPh	−2.6
5	MeSH	−5.0
6	NH_3	+22.5
7	MeOH	+8.6
8	PH_3	+0.2
9	$HPMe_2$	+16.1

[a] Negative reaction enthalpy denotes the preference for the heterolytic splitting isomer.

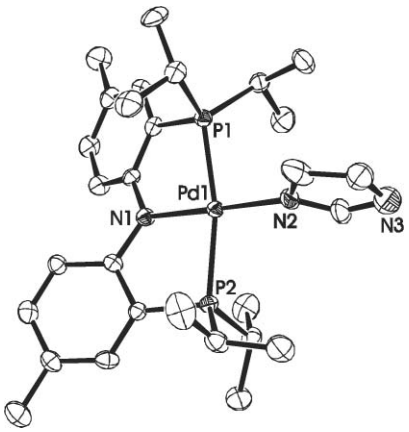

Fig. 4 ORTEP drawing (50% probability ellipsoids) of **7b-Barf** showing selected atom labelling. Hydrogen atoms, the rotational disorder of imidazole, the disordered toluene solvent molecule, and the BAr^F_4 anion are omitted for clarity. Selected bond distances (Å) and angles (°) follow: Pd1–P1, 2.2971(13); Pd1–P2, 2.2983(14); Pd1–N1, 2.008(4); Pd1–N2, 2.052(5); P1–Pd1–P2, 166.26(5); N1–Pd1–N2, 178.75(19).

Table 1 summarizes the enthalpic data obtained from the DFT calculations. Because this is a comparison between two isomers of broadly similar structure, entropic differences are likely relatively unimportant. Our computational results are largely consistent with the observed experimental data. Ammonia and imidazole are computed to prefer the simple adduct while MeSH (as a model for PhSH and $PhCH_2SH$), H_2, and the alkynes favour heterolytic splitting. The situation is somewhat divergent with phosphines: the two isomers arising from PH_3 are calculated to be essentially isothermic, but $HPMe_2$ strongly favours the simple adduct, just as observed experimentally with $HPCy_2$. Interestingly, the calculations also show that the hypothetical heterolytic splitting product is preferred for CH_4. Methanol is computed to favour a simple adduct. In experimental studies, ethanol failed to displace triflate and no adduct was observed.

On the viability of the Pd(IV) isomer and mechanism. Besides the two isomers already discussed, another conceivable structure for the adduct of HX to $[(PNP)Pd]^+$ is $[(PNP)Pd(H)(X)]^+$ with a Pd(IV) center. We evaluated the possibility of a Pd(IV) isomer for the case of H_2 (Scheme 4). We were unable to locate a minimum corresponding to the singlet **2c**; a triplet minimum for **2c** was found to lie 32 kcal mol^{-1} above the dihydrogen complex **2b** and thus

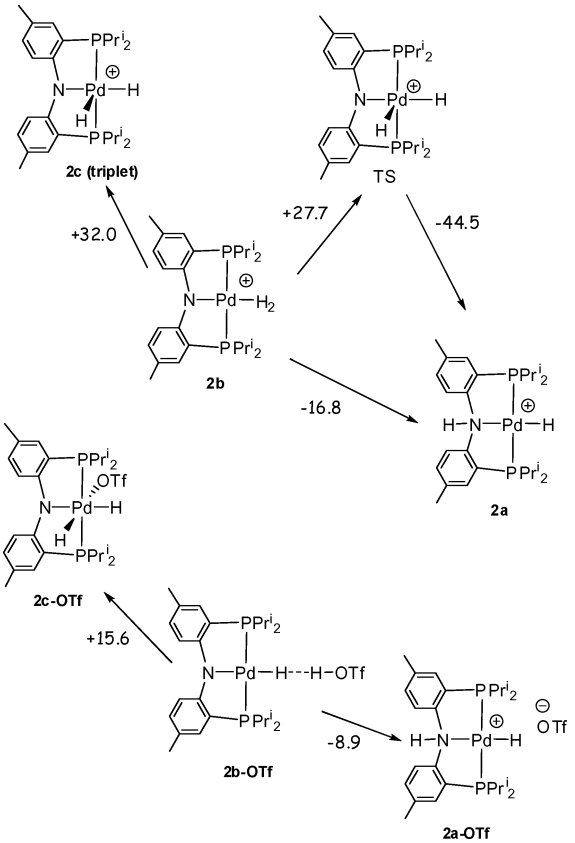

Scheme 4 Transformations among different isomers resulting from addition of H_2 to $[(PNP)Pd]^+$ (top) or (PNP)PdOTf (**1**, bottom) and the enthalpies of transformation calculated by DFT (shown over arrows).

49 kcal mol^{-1} above **2a**. If triflate is included in the calculations, a singlet minimum for $(PNP)Pd(H)_2(OTf)$ (**2c-OTf**) can be located 24.5 kcal mol^{-1} above the ground state **2a-OTf** (Scheme 4) and 15.6 kcal mol^{-1} above **2b-OTf**. While we have only analyzed this for the case of H_2, the rather large energy differences involved suggest that the five-coordinate Pd(IV) species, $[(PNP)Pd(H)(X)]^+$, are not viable products here.

We have also considered possible mechanisms for the formation of the heterolytic splitting products. Direct transfer of proton to N of PNP in (PNP)PdOTf from an H–X substrate appears improbable, especially for the H–X substrates of lower Brønsted acidity. The N in (PNP)PdCl is a weak enough base that it is protonated by HCl only reversibly (under vacuum).[13] Complex **1** is an even weaker Brønsted base and all of the substrates involved are weak Brønsted acids. An adduct $[(PNP)Pd(HX)]^+$ is likely initially formed *via* displacement of the triflate by the H–X ligand. We investigated the intramolecular isomerization of $[(PNP)Pd(H_2)]^+$ into $[(PN(H)P)PdH]^+$ with the help of a potential energy scan where the H–Pd–H angle was varied incrementally (5°) from 28° to 128°. As it was mentioned above, no minimum corresponding to a Pd(IV) $[(PNP)Pd(H_2)]^+$ structure was found along this path. The highest energy point was located at 27.7 kcal mol^{-1} above $[(PNP)Pd(H_2)]^+$, corresponding to an approximately square-pyramidal transition-state dihydride structure (Scheme 4, ∠H–Pd–H = 108°). While we cannot exclude the possibility of Pd(IV) intermediates or of concerted H-X cleavage for all substrates, we hypothesize that a more likely mechanism entails

Table 2 DFT calculated proton affinities at N_{PNP} of various (PNP)PdX compounds, as well as the Pd–N distances in (PNP)PdX and Pd–NH distance in $[(PN(H)P)PdX]^+$

#	X	PA/kcal mol^{-1}[a]	d(M–N)/Å	d(M–NH)/Å
1	CH_3	254.2	2.116	2.211
2	H	253.6	2.107	2.192
3	NH_2	251.1	2.082	2.160
4	PH_2	250.4	2.109	2.207
5	SMe	249.1	2.076	2.163
6	OMe	248.2	2.055	2.129
7	Cl	243.6	2.041	2.111

[a] PA = $-\Delta H$ of protonation.

proton transfer from a coordinated H_2 (or another HX) to N of PNP with the assistance of (catalytic) exogenous Brønsted base. This hypothesis dovetails the computational finding (*vide supra*) that triflate deprotonates **2b**. We do not know the exact nature of the exogenous base in each of the cases of heterolytic splitting, but it is logical to suggest that triflate, free H–X, adventitious impurities (*e.g.*, water), or neutral (PNP)PdX compounds are candidates of a varying degree of likelihood in each case.

Proton affinities. From another perspective, the three possible isomers resulting from addition of H–X to $[(PNP)Pd]^+$ are three different outcomes of protonation of (PNP)PdX: (a) at N_{PNP}, (b) at X, and (c) at Pd (Scheme 5). The lack of observed Pd(IV) products (and the DFT results concerning **2c**) indicate that Pd in (PNP)PdX is not a thermodynamically competitive protonation site in any of the cases under consideration. Protonation at X in (PNP)PdX appears to be preferred where X retains a lone pair and is a relatively strong base (phosphide or amide). However, it is necessary to point out that the variation of the basicity of X also affects the basicity of the N site in (PNP)PdX. We have calculated the gas phase proton affinities of the N site in several (PNP)PdX (Table 2) and found that they span a range of over 10 kcal mol^{-1}.

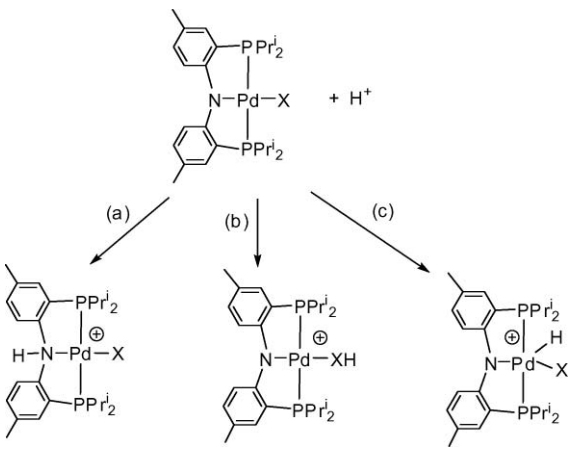

Scheme 5 Possible sites of protonation of (PNP)PdX.

Table 2 also lists the corresponding Pd–N_{PNP} distances in (PNP)PdX and in $[(PN(H)P)PdX]^+$. The increase in the Pd–N bond distance *trans* to X can be taken as a measure of the *trans* influence of X. There is a qualitative correlation between the increasing *trans* influence of X (increasing Pd–N_{PNP} distances) and the increasing proton affinity of N in (PNP)PdX, with NH_2 being slightly anomalous. NH_2 displays a weaker apparent *trans* influence than could be expected based on its effect on the proton affinity of N_{PNP}.

***N*- and *C*-bound imidazole.** Sini, Eisenstein, and Crabtree calculated that binding of parent imidazole to $[MCl_3]^-$ (M = Ni, Pd, Pt) and to a few other Pt(II) fragments favours *C*-binding *vs.* *N*-binding.[18] The *C*-bound tautomer is the simplest *N*-heterocyclic carbene. We saw no experimental evidence for the *C*-bound form (**7d**, Scheme 6), and computed that **7d** lies 15.0 kcal mol^{-1} higher in enthalpy than the observed *N*-bound isomer **7b**.

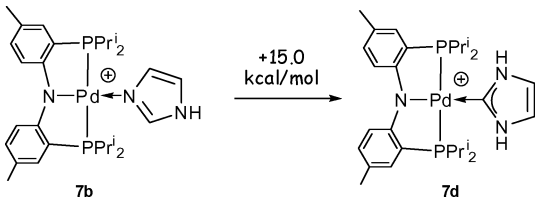

Scheme 6 Isomeric *N*-bound (**7b**) and *C*-bound (**7d**) imidazole complexes and the calculated enthalpy of isomerization (over the arrow).

Conclusions

In conclusion, we have demonstrated that the $[(PNP)Pd]^+$ fragment is capable of heterolytic cleavage of certain H–X bonds, such as in thiols, H_2, or an alkyne. On the other hand, H–X cleavage was disfavoured *vs.* simple coordination of H–X in cases where X^- is a relatively strong base with at least two lone pairs (RO^-, R_2N^-, R_2P^-). DFT calculations suggest that both of these outcomes are favored over the oxidative addition of H–X to the Pd center.

Experimental

General considerations

Unless specified otherwise, all manipulations were performed under an argon atmosphere using standard Schlenk line or glovebox techniques. Ethyl ether, C_6D_6, pentane, toluene, were dried over NaK/Ph_2CO/18-crown-6, distilled or vacuum transferred and stored over molecular sieves in an Ar-filled glovebox. Fluorobenzene was dried over and distilled from CaH_2. All other reagents and solvents were degassed and stored over 4A molecular sieves in a glovebox prior to use. Complex **1** was prepared according to published procedures.[18] The syntheses and characterization of complexes **2x**,[13] **8b-OTf**,[14] and **8x**[14] have been reported elsewhere. All other chemicals were used as received from commercial vendors. NMR spectra were recorded on a Varian iNova 400 (^{1}H NMR, 399.755 MHz; ^{13}C NMR, 100.518 MHz; ^{31}P NMR, 161.822 MHz) spectrometer. Chemical shifts are reported in δ (ppm). For ^{1}H and ^{13}C NMR spectra, the residual solvent peak was used as an internal reference. ^{31}P NMR spectra were referenced externally using 85% H_3PO_4 at δ 0 ppm. Elemental analyses were performed by CALI Labs, Inc. located in Parsippany, NJ, USA.

Computational details

The DFT calculations were carried out using the mPW1PW91 functional implemented in Gaussian 03.[19] All structures were fully optimized twice, first using bases set BS1 and then BS2. The basis

set BS1 included: SDD (associated with the corresponding ECP) for Pd, 6-31G(d) for all N, O, F, P, S atoms, 6-31G(p) for the hydrogen atom of HX, 6-31G for the *i*-Pr groups, and 6-31G(d) for all other atoms. The basis set BS2 included: SDD (associated with the corresponding ECP) for Pd, 6-311+G(d) for all N, O, F, P, S atoms and metal-bonded carbon atoms, 6-31G(p) for the hydrogen atom of HX, and 6-31G(d) for all other atoms. The C=C carbon atoms of C_2H_2 and HCCPh were modelled at the 6-311+G(d) level in BS2. The nature of all stationary points was verified by frequency calculations at the mPW1PW91/BS1 level. All reported enthalpies were obtained by adding thermal corrections provided by the frequency calculations to the corresponding electronic energies from the mPW1PW91/BS2 geometry optimizations.

X-Ray crystallography

X-Ray data collection for **2a-OTf** was carried out at room temperature (low temperature apparatus was not available) on a CAD-4 Turbo diffractometer equipped with Mo Kα radiation.[20] For **3x**, **6x**, and **7b-Barf**, All operations were performed on a Bruker-Nonius Kappa Apex2 diffractometer, using graphite-monochromated Mo Kα radiation. All diffractometer manipulations, including data collection, integration, scaling, and absorption corrections were carried out using the Bruker Apex2 software.[21] All four structures were solved by direct methods (SIR92).[22] Full-matrix least squares refinements were carried out using the Oxford University Crystals for Windows system.[23] Additional crystallographic details are available in the Electronic Supporting Information in the form of CIF files and descriptions of data collection, solution and refinement for each structure.

Preparations

[(PN(H)P)PdH]$^+$OTf$^-$ (2a-OTf). (PNP)PdOTf (**1**) (68 mg, 0.10 mmol) was dissolved in 3 mL C_6D_6 in a sealed reaction tube, and 1 atm H_2 was charged in. The reaction mixture was stirred at ambient temperature for 10 min, and it was found that the solution became colourless gradually. All of the volatiles were removed under vacuum, and the pure colourless product was obtained after recrystallization from fluorobenzene/isooctane mixture. (Yield: 42 mg, 60%). ^{1}H NMR (C_6D_6): δ 10.57 (s, 1 H, N-*H*), 7.59 (d, 2 H, Ar-*H*), 7.04 (s, 2 H, Ar-*H*), 6.94 (d, 2 H, Ar-*H*), 2.55 (m, 2 H, C*H*Me$_2$), 2.08 (s, 6 H, Ar-*Me*), 1.96 (m, 2 H, C*H*Me$_2$), 1.14 (app q., 12 H, J = 9 Hz, CH*Me*$_2$), 0.91 (app q., 6 H, J = 9 Hz, CH*Me*$_2$), 0.64 (app q., 6 H, J = 8 Hz, CH*Me*$_2$), −12.04 (s, 1H, Pd–H). ^{13}C{^{1}H} NMR (C_6D_6): δ 147.8 (t, J_{C-P} = 9 Hz), 137.3, 133.6, 133.1, 130.8 (t, J_{C-P} = 7 Hz), 125.9, 26.5 (t, J_{C-P} = 12 Hz), 23.3 (t), 20.4, 20.0, 19.3, 19.0, 18.4. ^{31}P{^{1}H} NMR (C_6D_6): δ 57.4. ^{19}F NMR (C_6D_6): δ −80.6.

(PNP)PdH (2x). (PNP)PdOTf (**1**) (20 mg, 29 μmol) was dissolved in about 0.6 mL C_6D_6 in a J. Young tube. The solution was frozen and the headspace evacuated and back filled with hydrogen gas (1 atm). The reaction mixture was placed in a 50 °C oil bath for 3 h and the purple solution became colourless gradually. Analysis by both ^{31}P NMR and ^{1}H NMR indicated the formation of **2a-OTf**. Triethylamine (7 μL, 45 μmol) was added and the color changed to yellow immediately. NMR analysis indicated complete conversion to **2x**.

[(PN(H)P)Pd–C≡CTol]$^+$OTf$^-$ (3a-OTf). (PNP)PdOTf (**1**) (30 mg, 0.043 mmol) was dissolved in ether and *p*-tolylacetylene (5.3 μL, 0.043 mmol) was added. Immediately upon mixing the color changed from dark blue to clear pale yellow. The reaction was allowed to stir for 10 min at ambient temperature. The volatiles were removed *in vacuo* and washed with cold pentane. (Yield: 27 mg, 82%) ^{1}H NMR (C_6D_6): δ 11.4 (s, 1 H, N-*H*), 7.51 (m, 2 H), 7.36 (d, 2 H, J = 8 Hz, Ar-*H*), 7.00 (m, 2 H), 6.90 (d, 2 H, J = 8 Hz, Ar-*H*), 6.73 (d, 2 H, J = 8 Hz, Ar-*H*), 2.84 (m, 2 H, C*H*Me$_2$), 2.27 (m, 2 H, C*H*Me$_2$), 2.08 (s, 3 H, *p*-C*H*$_3$), 2.04 (s, 6 H, Ar–C*H*$_3$), 1.29 (m, 12 H, CH*Me*$_2$), 0.92 (m, 12 H, CH*Me*$_2$). ^{13}C{^{1}H} (C_6D_6): δ 148.6 (t, J = 9 Hz), 138.7, 136.3, 133.5, 132.8, 131.4, 129.7, 129.6, 125.8 (t, J = 3 Hz), 125.6, 120.2 (t, J = 4 Hz), 116.2 (t, J = 15 Hz), 77.6, 27.6 (t, J = 11 Hz), 24.7, 21.6, 20.9, 20.1, 18.8, 18.1. ^{31}P{^{1}H} NMR (C_6D_6): δ 47.7. ^{19}F NMR (C_6D_6): δ −80.6. Elem. anal. calcd for $C_{36}H_{48}F_3NO_3P_2PdS$: C 54.04, H 6.05. Found: C 54.12, H 5.95.

(PNP)Pd–C≡CTol (3x). Compound **3a-OTf** (60 mg, 0.075 mmol) was dissolved in toluene and K_2CO_3 (15 mg, 0.10 mmol) was added. The reaction was allowed to stir overnight at ambient temperature. The solution was filtered though Celite and the volatiles were removed under vacuum. Yellow/orange crystals were obtained from recrystallization of the residue from a 1 : 3 toluene–pentane mixture. (Yield: 32 mg, 61%) ^{1}H NMR (C_6D_6): δ 7.78 (d, 2 H, J = 8 Hz, Ar-*H*), 7.59 (d, 2 H, J = 8 Hz, Ar-*H*), 7.01 (d, 2 H, J = 8 Hz, Ar-*H*), 6.85 (m, 4 H), 2.27 (m, 4 H, C*H*Me$_2$), 2.16 (s, 6 H, Ar–C*H*$_3$), 2.09 (s, 3 H, *p*-C*H*$_3$), 1.45 (dvt, 12 H, CH*Me*$_2$), 1.10 (dvt, 12 H, CH*Me*$_2$). ^{13}C{^{1}H} NMR C_6D_6: δ 162.4 (t, J = 11 Hz), 133.6, 133.2, 131.6, 129.7, 127.5, 125.4, 120.9, 116.8 (t), 116.4 (t), 25.6 (t, J = 13 Hz), 21.9, 21.0, 19.5, 18.8. ^{31}P{^{1}H} NMR C_6D_6: δ 50.6. Elem. anal. calcd for $C_{35}H_{47}NP_2Pd$: C 64.66, H 7.29. Found: C 64.76, H 7.44.

[(PN(H)P)Pd-SPh]$^+$OTf$^-$ (4a-OTf). (PNP)PdOTf (**1**) (50 mg, 0.073 mmol) was dissolved in toluene then benzenethiol (8.5 μL, 0.082 mmol) was added to it. The solution immediately changed from dark blue to a dark red upon mixing. The solution was allowed to stir for 10 min then the volatiles were removed *in vacuo*. A purple/red powder was obtained by recyrstallization of the residue from a toluene–pentane mixture. (Yield: 43 mg 78%). ^{1}H NMR (C_6D_6): δ 11.3 (s, 1 H, N-*H*), 8.04 (d, 2 H, J = 8 Hz, Ar-*H*), 7.40 (d, 2 H, J = 8 Hz, Ar-*H*), 6.97–6.83 (m, 7 H), 2.50 (m, 2 H, C*H*Me$_2$), 2.24 (m, 2 H, C*H*Me$_2$), 2.02 (s, 6 H, Ar-C*H*$_3$), 1.26–1.08 (m, 24 H, CH*Me*$_2$). ^{13}C{^{1}H} NMR (C_6D_6): δ 148.8 (t, J = 8 Hz, *C*–N), 145.3, 138.6 (t, J = 3 Hz), 133.4 (d, J = 6 Hz), 133.0, 129.9, 129.6, 128.9, 125.9, 127.0, 27.4 (t, J_{C-P} = 11 Hz, C*H*Me$_2$), 25.4 (t, J_{C-P} = 12 Hz, C*H*Me$_2$), 20.9 (Ar-*C*H$_3$), 19.0 (Ar-*C*H$_3$), 18.7 (CH*Me*$_2$), 18.5 (CH*Me*$_2$), 1.76. ^{31}P{^{1}H} NMR (C_6D_6): δ 41.0. ^{19}F NMR (C_6D_6): −80.5. Elem. anal. calcd for $C_{33}H_{46}F_3NO_3P_2PdS_2$: C 49.90, H 5.84. Found: C 51.68, H 6.04.

(PNP)Pd–S-Ph (4x). Compound **4a-OTf** (30 mg, 0.038 mmol) was dissolved in ether and K_2CO_3 (5.7 mg, 0.040 mmol) was added. The mixture was allowed to stir at ambient temperature overnight. The solution was filtered through Celite to remove insolubles and the volatiles were removed *in vacuo*. (Yield: 16 mg, 66%). ^{1}H NMR (C_6D_6): δ 7.91 (d, 2 H, J = 8 Hz, Ar-*H*), 7.70 (d, 2 H, J = 2 Hz, Ar-*H*), 7.05 (t, 2 H, J = 8 Hz, Ar-*H*), 6.91–6.80 (m, 5 H), 2.18 (m, 4 H, C*H*Me$_2$), 2.13 (s, 6 H, Ar-C*H*$_3$), 1.31 (dvt, 12 H, J = 8 Hz,

CH*Me*$_2$), 1.07 (dvt, 12 H, J = 8 Hz, CH*Me*$_2$). ^{13}C{^{1}H} NMR (C_6D_6): δ 162.2 (t, J = 10 Hz, *C*–N), 149.9, 133.2, 128.0, 125.9 (t), 122.3, 120.8, 120.6, 116.6 (t, J = 5 Hz), 25.7 (t, $J_{C\text{-}P}$ = 12 Hz, C*H*Me$_2$), 21.0 (Ar-*C*H$_3$), 19.0 (CH*Me*$_2$), 18.3 (CH*Me*$_2$). ^{31}P{^{1}H} NMR (C_6D_6): δ 45.7. Elem. anal. calcd for $C_{32}H_{45}NP_2PdS$: C 59.67, H 7.04. Found: C 59.61, H 7.12.

[(PN(H)P)Pd-SBn]$^+$OTf$^-$ (5a-OTf). (PNP)PdOTf (**1**) (60 mg, 0.088 mmol) was dissolved in C_6D_6; then benzylthiol (12 μL, 0.10 mmol) was added and the solution changed from a bright blue to a clear red upon mixing. The volatiles were removed under vacuum and the solid was washed with pentane resulting in a red/purple solid. (Yield: 59 mg, 88%) ^{1}H NMR (C_6D_6): δ 11.2 (s, 1 H, N-*H*), 7.58 (d, 2 H, J = 8 Hz), 7.41 (d, 2 H, J = 8 Hz), 7.29 (t, 2 H, J = 8 Hz), 7.03 (t, 1 H, J = 8 Hz), 6.95 (s, 2 H), 6.85 (d, 2 H, J = 8 Hz), 3.88 (s, 2 H, S–C*H*$_2$), 2.73 (m, 2 H, C*H*Me$_2$), 2.19 (m, 2 H, C*H*Me$_2$), 2.00 (s, 6 H, Ar-C*H*$_3$), 1.31–1.14 (m, 24 H, CH*Me*$_2$). ^{13}C{^{1}H} NMR (C_6D_6): δ 148.8 (t, J = 9 Hz), 144.0, 138.5, 133.5, 129.9 (t), 129.7, 129.5, 129.3, 127.6, 127.3, 126.1, 29.5, 28.0 (t, J = 12 Hz), 25.4 (t, J = 12 Hz), 21.2, 19.7, 19.0, 18.7, 18.3. ^{31}P{^{1}H} NMR (C_6D_6): δ 40.6. ^{19}F NMR (C_6D_6): δ –80.5. Elem. anal. calcd for $C_{34}H_{48}F_3NO_3P_2PdS_2$: C 50.53, H 5.99. Found: C 50.45, H 6.06.

(PNP)Pd-SBn (5x). Compound **5a-OTf** (30 mg, 0.037 mmol) was dissolved in a 1 : 1 toluene/ether mixture and K_2CO_3 (7 mg, 0.050 mmol) was added. The mixture was allowed to stir at ambient temperature overnight and the colour changed to a lighter orange/red. The solution was filtered through Celite to remove the insolubles and the volatiles were removed *in vacuo*. (Yield: 14 mg, 57%) ^{1}H NMR (C_6D_6): δ 7.74 (d, 2 H, J = 8 Hz), 7.63 (d, 2 H, J = 8 Hz), 7.22 (t, 2 H, J = 8 Hz), 7.08 (t, 1 H, J = 8 Hz), 6.98 (s, 2 H), 6.80 (d, 2 H, 8 Hz), 3.88 (s, 2 H, S–C*H*$_2$), 2.31 (m, 4 H, C*H*Me$_2$), 2.16 (s, 6 H, Ar-C*H*$_3$), 1.38 (dvt, 12 H, CH*Me*$_2$), 1.11 (dvt, 12 H, CH*Me*$_2$). ^{13}C{^{1}H} NMR (C_6D_6): δ 162.1 (t, J = 10 Hz), 146.0, 133.2, 132.9, 129.4, 128.8, 126.4, 125.4 (t, J = 3 Hz), 120.5 (t, J = 18 Hz), 116.4 (t, J = 6 Hz), 36.6 (t, J = 3 Hz), 25.8 (t, J = 11 Hz), 20.9, 18.9, 18.3. ^{31}P{^{1}H} NMR (C_6D_6): δ 44.7. Elem. anal. calcd for $C_{33}H_{47}NP_2PdS$: C 60.22, H 7.20. Found: C 60.09, H 7.13.

[(PNP)Pd(HPCy$_2$)]$^+$OTf$^-$ (6b-OTf). (PNP)PdOTf (**1**) (100 mg, 0.15 mmol) was dissolved in toluene (2 mL) followed by addition of PHCy$_2$ (30 μL, 0.15 mmol). The solution was stirred for 20 min. Stirring was ceased and the solution was allowed to stand overnight. Purple crystals were collected (110 mg, 86% yield). ^{1}H NMR (d$_6$-acetone): δ 7.05 (d, 2 H, J = 9 Hz, Ar-*H*), 6.96 (s, 1 H), 6.73 (d, 2 H, J = 8 Hz, Ar-*H*), 4.54 (d mult, 1 H, J_{HP} = 352, P-*H*), 2.63 (br, 4 H, C*H*Me$_2$), 2.14–1.17 (m, 22 H, PH*Cy*$_2$) 1.97 (s, 6 H, Ar-*Me*), 1.19 (app q, 12 H, J = 8 Hz, CH*Me*$_2$), 1.01 (app q, 12 H, J = 7 Hz, CH*Me*$_2$). ^{13}C NMR (d$_6$-acetone): δ 160.7(*C*–N), 134.1, 132.3, 128.1 (t), 117.6 (t, J_{CP} = 20 Hz, *C*–P), 116.4, 37.2 (d, J_{CP} = 25 Hz, *C*–P), 34.0 (m), 27.5 (m), 26.0, 25.6 (m, *C*HMe$_2$), 20.2, 19.6, 17.7. ^{31}P{^{1}H} NMR (d$_6$-acetone): δ 60.8 (br), 9.21 (t, J_{PP} = 34 Hz). ^{19}F NMR (d$_6$-acetone): δ 80.0. Elem. anal. calcd for $C_{39}H_{63}F_3NO_3PdP_3S$: C 53.09, H 7.19. Found: C 52.98, H 7.23.

(PNP)Pd-PCy$_2$ (6x). Compound **6b-OTf** was dissolved in fluorobenzene (3 mL). KOBu^t (9.5 mg, 0.085 mmol) was added and the solution stirred for 90 min. The solution had turned from purple to orange. The solution was filtered through a pad of Celite. The volatiles were removed under vacuum. The residue was dissolved in pentane and placed in the –35 °C freezer. Brown orange crystals were collected after standing overnight (48 mg, 77% yield). ^{1}H NMR (C_6D_6): δ 7.64 (d, 2 H, J = 8 Hz, Ar-*H*), 6.87 (s, 2 H, Ar-*H*), 6.84 (d, 2 H, J = 9 Hz, Ar-*H*), 2.67–1.33 (m, 22 H, P*Cy*$_2$), 2.27 (m, 4 H, C*H*Me$_2$), 2.20 (s, 6 H, Ar-*Me*), 1.43 (br, 12 H, CH*Me*$_2$), 1.11 (br, 12 H, CH*Me*$_2$). ^{13}C NMR (C_6D_6): δ 160.4(*C*–N), 132.6, 132.5, 123.9 (t), 120.4 (t, J_{CP} = 19 Hz, *C*–P), 115.7, 41.4 (d, J_{CP} = 33 Hz, *C*–P), 36.3 (m), 28.4 (m), 27.3, 24.6 (t, J_{CP} = 11 Hz, *C*HMe$_2$), 20.8, 19.7, 17.3. ^{31}P{^{1}H} NMR (C_6D_6): δ 37.4 (d, 21 Hz), 17.6 (t, 21 Hz). Elem. anal. calcd for $C_{38}H_{62}NPdP_3$: C 62.33, H 8.53. Found: C 62.28, H 8.48.

[(PNP)Pd(imidazole)]$^+$BAr$^F_4{}^-$ (7b-Barf). (PNP)PdOTf (**1**) and imidazole (4.9 mg, 0.073 mmol) were dissolved in fluorobenzene (2 mL). The solution changed in color from dark purple to a purple pink colour. This solution was stirred for 1 h. $NaBArF_{24}$ was added and solution stirred an additional hour. The solution was filtered through a pad of Celite. Volatiles were removed under vacuum. The residue was washed with iso-octane then dried under vacuum resulting in a purple powder (99 mg, 92% yield). ^{1}H NMR (d$_6$-acetone): δ 8.62 (s, 1 H), 7.90 (br, 1 H), 7.80 (s, 8 H, $BArF_{24}$), 7.68 (s, 4 H, $BArF_{24}$), 7.52 (s, 1 H), 7.42 (d, 2 H, J = 8 Hz, Ar-*H*), 7.20 (br, 1 H), 7.14 (br, 2 H, Ar-*H*), 6.97 (d, 2 H, J = 8 Hz, Ar-*H*), 2.64 (m, 4 H, C*H*Me$_2$), 2.21 (s, 6 H, Ar-*Me*), 1.20 (app q, 12 H, J = 8 Hz, CH*Me*$_2$), 1.08 (app q, 12 H, J = 8 Hz, CH*Me*$_2$). ^{13}C NMR (d$_6$-acetone): δ 162.7 (q, J_{CB} = 48 Hz, *C*–B), 162.5 (t, J = 11 Hz, *C*–N), 139.4 (imidazole), 135.6 (BArF), 133.8, 133.7, 130.8 (imidazole), 130.1 (qm, J_{CF} = 31 Hz, *C*–CF$_3$), 127.9 (t), 125.5 (q, J_{CF} = 272 Hz, *C*F$_3$), 120.6 (imidazole), 118.5 (BArF), 117.3 (t, J_{CP} = 21 Hz, *C*–P), 117.0 (t), 24.5, (t, J_{CP} = 12 Hz, *C*HMe$_2$), 20.3, 18.3, 17.7. ^{31}P{^{1}H} NMR (d$_6$-acetone): δ 52.3. ^{19}F NMR (d$_6$-acetone): δ 64.9. Elem. anal. calcd for $C_{61}H_{56}BF_{24}N_3PdP_2$: C 49.97, H 3.85, N 2.87. Found: C 49.78, H 3.83, N 2.91.

Acknowledgements

We are grateful for the support of this work by the US National Science Foundation (CHE-0944634), the Sloan Foundation, the Dreyfus Foundation, and the Welch Foundation. We also thank the National Science Foundation for the partial support of this work through grant CHE-0521047 for the purchase of a new X-ray diffractometer at Brandeis University. We are grateful to Yanjun Zhu for assistance with collection of some of the NMR data.

References

1 (*a*) R. H. Crabtree, *The Organometallic Chemistry of the Transition Metals*, Wiley-Interscience, New York, 2001; (*b*) P. W. N. M. van Leeuwen, *Homogeneous Catalysis: Understanding the Art*, Kluwer Academic Publishers, Dordrecht, Boston, London, 2004.
2 G. D. Frey, V. Lavallo, B. Donnadieu, W. W. Schoeller and G. Bertrand, *Science*, 2007, **316**, 439.
3 C. A. Sandoval, T. Ohkuma, K. Muñiz and Ryoji Noyori, *J. Am. Chem. Soc.*, 2003, **125**, 13490.
4 K. Abdur-Rashid, S. E. Clapham, A. Hadzovic, J. N. Harvey, A. J. Lough and R. H. Morris, *J. Am. Chem. Soc.*, 2002, **124**, 15104.
5 C. B. Pamplin and P. Legzdins, *Acc. Chem. Res.*, 2003, **36**, 223.
6 (*a*) L. M. Slaughter, P. T. Wolczanski, T. R. Klinckman and T. R. Cundari, *J. Am. Chem. Soc.*, 2000, **122**, 7953; (*b*) J. L. Bennett and P. T. Wolczanski, *J. Am. Chem. Soc.*, 1997, **119**, 10696; (*c*) C. P. Schaller, C. C. Cummins and P. T. Wolczanski, *J. Am. Chem. Soc.*, 1996, **118**, 591.
7 D. J. Mindiola, *Acc. Chem. Res.*, 2006, **39**, 813.

8 For reviews on the chemistry of diarylamido-based PNP complexes, see: (*a*) L.-C. Liang, *Coord. Chem. Rev.*, 2006, **250**, 1152; (*b*) O. V. Ozerov, in *The Chemistry of Pincer Compounds*, D. Morales-Morales and C. Jensen, ed., Elsevier, Amsterdam, 2007, pp. 287–309; (*c*) D. J. Mindiola, B. C. Bailey and F. Basuli, *Eur. J. Inorg. Chem.*, 2006, 3135.
9 D. W. Stephan, *Dalton Trans.*, 2009, 3129.
10 J. Zhang, G. Leitus, Y. Ben-David and D. J. Milstein, *J. Am. Chem. Soc.*, 2005, **127**, 10840.
11 L. Fan, L. Yang, C. Guo, B. M. Foxman and O. V. Ozerov, *Organometallics*, 2004, **23**, 4778.
12 L. Fan and O. V. Ozerov, *Chem. Commun.*, 2005, 4450.
13 L. Fan, B. M. Foxman and O. V. Ozerov, *Organometallics*, 2004, **23**, 326.
14 C. M. Fafard, D. Adhikari, B. M. Foxman, D. J. Mindiola and O. V. Ozerov, *J. Am. Chem. Soc.*, 2007, **129**, 10318.
15 M. A. Zhuravel, D. S. Glueck, L. N. Zakharov and A. L. Rheingold, *Organometallics*, 2002, **21**, 3208.
16 M.-A. David, D. K. Wicht, D. S. Glueck, G. P. A. Yap, L. M. Liable-Sands and A. L. Rheingold, *Organometallics*, 1997, **16**, 4768.
17 O. V. Ozerov, C. Y. Guo, L. Fan and B. M. Foxman, *Organometallics*, 2004, **23**, 5573.
18 G. Sini, O. Eisenstein and R. H. Crabtree, *Inorg. Chem.*, 2002, **41**, 602.
19 (*a*) M. J. Frisch, G. W. Trucks, H. B. Schlegel, G. E. Scuseria, M. A. Robb, J. R. Cheeseman, J. A. Montgomery, Jr., T. Vreven, K. N. Kudin, J. C. Burant, J. M. Millam, S. S. Iyengar, J. Tomasi, V. Barone, B. Mennucci, M. Cossi, G. Scalmani, N. Rega, G. A. Petersson, H. Nakatsuji, M. Hada, M. Ehara, K. Toyota, R. Fukuda, J. Hasegawa, M. Ishida, T. Nakajima, Y. Honda, O. Kitao, H. Nakai, M. Klene, X. Li, J. E. Knox, H. P. Hratchian, J. B. Cross, V. Bakken, C. Adamo, J. Jaramillo, R. Gomperts, R. E. Stratmann, O. Yazyev, A. J. Austin, R. Cammi, C. Pomelli, J. Ochterski, P. Y. Ayala, K. Morokuma, G. A. Voth, P. Salvador, J. J. Dannenberg, V. G. Zakrzewski, S. Dapprich, A. D. Daniels, M. C. Strain, O. Farkas, D. K. Malick, A. D. Rabuck, K. Raghavachari, J. B. Foresman, J. V. Ortiz, Q. Cui, A. G. Baboul, S. Clifford, J. Cioslowski, B. B. Stefanov, G. Liu, A. Liashenko, P. Piskorz, I. Komaromi, R. L. Martin, D. J. Fox, T. Keith, M. A. Al-Laham, C. Y. Peng, A. Nanayakkara, M. Challacombe, P. M. W. Gill, B. G. Johnson, W. Chen, M. W. Wong, C. Gonzalez and J. A. Pople, *GAUSSIAN 03 (Revision E.01)*, Gaussian, Inc., Wallingford, CT, 2004; (*b*) for additional references and technical details concerning the functionals and bases sets implemented in Gaussian 03, see: A. Frish, M. J. Frish and G. W. Trucks, *Gaussian 03 User's Reference*, Gaussian, Inc., Pittsburgh PA, 2003.
20 L. H. Straver, *CAD4-EXPRESS*, Enraf-Nonius, Delft, The Netherlands, 1992.
21 *Apex2, Version 2 User Manual, M86-E01078*, Bruker Analytical X-ray Systems, Madison, WI, 2006.
22 A. Altomare, G. Cascarano, G. Giacovazzo, A. Guagliardi, M. C. Burla, G. Polidori and M. Camalli, *J. Appl. Cryst.*, 1994, **27**, 435.
23 P. W. Betteridge, J. R. Carruthers, R. I. Cooper, K. Prout and D. J. Watkin, *J. Appl. Crystallogr.*, 2003, **36**, 1487.

